Synthesis of aluminum alloy 7075-graphite composites by milling processes and hot extrusion

R. Deaquino-Lara [a,b], I. Estrada-Guel [a], G. Hinojosa-Ruiz [c], R. Flores-Campos [a,d], J.M. Herrera-Ramírez [a], R. Martínez-Sánchez [a,*]

[a] Centro de Investigación en Materiales Avanzados (CIMAV), Laboratorio Nacional de Nanotecnología, Miguel de Cervantes No. 120, C.P. 31109, Chihuahua, Chih., Mexico
[b] Centro de Investigación y de Estudios Avanzados del IPN (CINVESTAV), Unidad Saltillo Carretera Saltillo-Monterrey km 13.5, C.P. 25000, Ramos Arizpe, Coah., Mexico
[c] Instituto Tecnológico de Saltillo (ITS), Blvd. Venustiano Carranza No. 2400, C.P. 25280, Saltillo, Coah., Mexico
[d] Departamento de Ingeniería, Tecnológico de Monterrey Campus Saltillo, Prol. Juan de la Barrera No. 1241 Ote., Col. Cumbres, C.P. 25270, Saltillo, Coah., Mexico

ARTICLE INFO

ABSTRACT

Aluminum alloy 7075 (Al_{7075}) and composites of Al_{7075} with different concentrations of graphite particles (Al_{7075}-G) were synthesized from elemental powders by a milling process. Milled products were consolidated by pressureless-sintering followed by hot extrusion. The mechanical properties of the sintered specimens were evaluated by tension tests and hardness measurements. Variation of Zn and graphite contents and their effect on mechanical properties was characterized. The results obtained show that the yield strength (σ_y), the maximum strength (σ_{max}) and the Vickers microhardness (μHV) were enhanced as a function of graphite particles content and milling time, but the elongation was reduced significantly in some cases.

© 2010 Elsevier B.V. All rights reserved.

1. Introduction

Due to their low density and good workability, aluminum (Al) alloys have a wide variety of industrial applications [1–8]. The 7XXX series Al alloys have received special attention in aerospace industries, because they provide the highest strength among all aluminum alloys [1]. These alloys offer a wide range of strength and ductility. They have been extensively used in aerospace and other structural applications and also for the development of Metal Matrix Composites (MMCs). Aluminum alloy 7075 (Al_{7075}), the most common alloy of this series, provides a good combination of strength, ductility, and toughness. The need to increase aluminum strength for structural applications in aerospace and aeronautic industries has motivated the study of Aluminum Matrix Composites (AMCs) [2–8]. Reinforcing the ductile aluminum matrix with stronger and stiffer second-phase reinforcements, like oxides, carbides and nitrides provides a combination of properties of both the metallic matrix and the ceramic reinforcement components resulting in improved physical and mechanical properties of the composite [2,3].

There are several fabrication techniques available to manufacture MMCs, which can be divided in two main types: solid state

processes [2–8] and liquid state process [4]. In the former, the mechanical alloying (MA) and mechanical milling (MM) are generally used to obtain excellent mechanical properties in MMCs. This is because during high-energy milling the powder particles are repeatedly flattened, cold welded, fractured and rewelded. After milling for a certain length of time, steady-state equilibrium is reached when a balance between the rate of welding, and the rate of fracturing is achieved. At this stage each particle contains substantially all of the starting materials, in the proportion they were mixed together [5,6]. The segregation effects are less and an homogeneous distribution of reinforcement particles into the composite can be obtained.

Recently, some researchers have demonstrated that employing graphite as reinforcement agent to produce Al-based composites by mechanical milling [6,7], increases the mechanical resistance of the composites. These particles are responsible of this improvement since their addition favors the refining of the powder particle size during the milling process [6,7], and promotes the mechanical alloying process acting as a process control agent (PCA).

The focus in this work was the microstructural and mechanical characterization of Al_{7075}-graphite composites produced by the dispersion of graphite particles (G) by milling processes. Also the Zn content in the composite was decreased in order to determine if the graphite addition could compensate the effect of Zn decrease. The yield strength (σ_y) and maximum strength (σ_{max}) of the composites were determined by tensile tests, and hardness was evaluated

* Corresponding author. Tel.: +52 614 439 11 46; fax: +52 614 439 48 23.
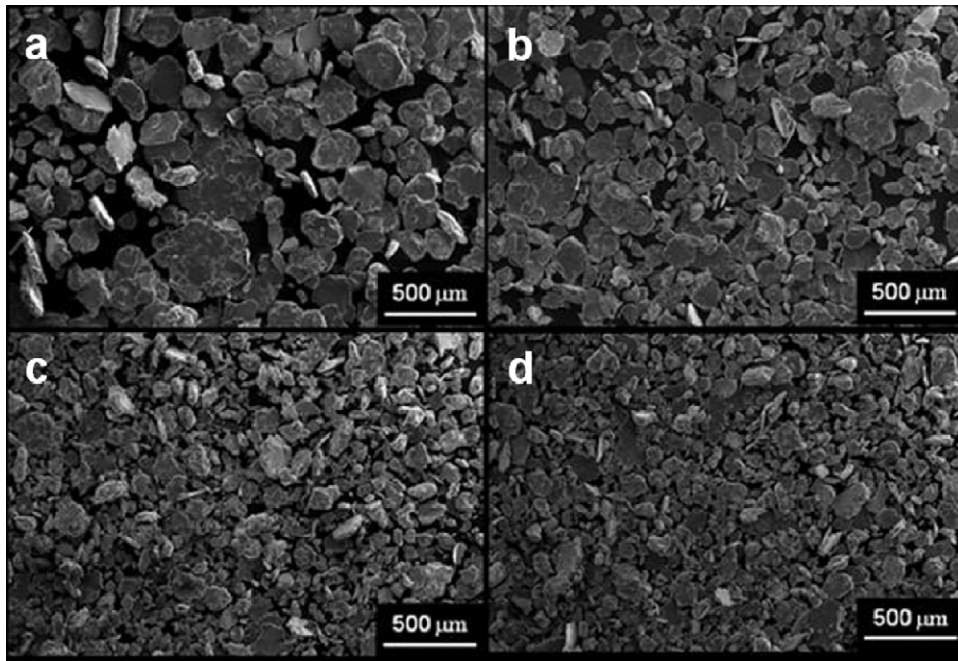*E-mail address:* roberto.martinez@cimav.edu.mx (R. Martínez-Sánchez).

Fig. 1. Morphology evolution in Al$_{7075}$ 3Zn sample as a function of graphite content, with 10 h of milling: (a) 0.0, (b) 0.5, (c) 1.0 and (d) 1.5% G.

by Vickers microhardness (μHV). Furthermore an analysis of the effect of graphite particles on mechanical properties is described.

2. Experimental procedure

The composite powders were manufactured by mixing simultaneously elemental powders in the appropriate percentage to obtain the aluminum alloy 7075 matrix and the selected graphite content [7]. Table 1 shows all chemical composition of the used composites, as well the theoretical density (ρ_{Theor}) calculated by the rule of mixtures. The purity of the G used was 99.9% and the average particle size was 38.33 μm, where 90% of those particles had a size <84 μm. The G were produced from graphite powder by mechanical milling in a high energy mill (SPEX-8000 M) during 8 h in an argon atmosphere [5–8].

Composite mixtures were blended during 5 min using the same equipment without grinding balls in order to obtain an homogeneous mixture, and then mechanically milled in a high energy ball mill (Simoloyer CM01) for 5 and 10 h in an argon atmosphere. Using this method, the formation of the Al$_{7075}$ alloy and the dispersion of graphite particles into the aluminum alloy matrix were achieved in the same process.

The milling device and the milling media used in the experiments were made from hardened steel. The milling ball-to-powder weight ratio was 14, and the total sample weight was 70 g for all the samples. Methanol was added as a process control agent (PCA) in amounts of 3 ml. Consolidated bulk products (40 mm in diameter) were prepared by pressing the milled powder at ~460 MPa for 2 min under uniaxial load. The pressed samples were then sintered in vacuum during 3 h at 823 K with a heating rate of 50 K/min. Sintered products were held during 0.5 h at 773 K and hot extruded into a rod with a diameter of 10 mm, using indirect extrusion with an extrusion ratio of 16. In order to study the effect of milling process over conventional powder metallurgy method, an additional sample in the as-mixed condition (not milled) and without G, but prepared by the same consolidation route, was employed as reference material (Al$_{7075}$ 5Zn0G-M).

The structural changes of powders during the milling process were determined by X-ray diffraction (XRD). A PANalytical X'Pert PRO diffractometer (40 kV, 35 mA) with Cu Kα radiation (λ = 0.15406 nm) was used for the measurements. The lattice parameter of the Al (Zn) solid solution was determined from the Al (1 1 1), (2 0 0), (2 2 0), (3 1 1) and (2 2 2) reflections. The crystallite size was determined by the Williamson–Hall formula [9,10]. SEM observations were done in a JEOL JSM6510-LV microscope operated at 20 kV.

Tension tests were carried out by pulling the samples along the longitudinal (extrusion) direction at room temperature in a MTS 810 universal testing machine with a load cell of 100 kN. The displacement rate was 0.016 mm/s. The yield strength (σ_y) was evaluated by the offset method at 0.2% of strain. For the tension tests, bone shaped samples were used in accordance with ASTM B557 M standard. Vickers microhardness (μHV) was evaluated in a Wilson TUKON microhardness tester, using a dwell time of 15 s and a maximum load of 200 g.

3. Results

3.1. Morphology

Fig. 1 presents some secondary electron SEM micrographs, showing the effect of the G content on the morphology of Al$_{7075}$ 3Zn particles for samples milled during 10 h. Notice that as the G content increases, the particle size decreases, indicating that the comminuting process is favored by the G content; this suggests that the graphite particles act as PCA [6,7]. Short milling times cause graphite agglomeration [11], which affects the final mechanical properties in Al-based composites. However, this problem was not observed in the composites synthesized in this work. This can be attributed to the long processing times used.

3.2. X-ray diffraction

Fig. 2 shows the XRD spectra of the Al$_{7075}$ alloy at different milling times. The diffraction peaks corresponding to Al, Zn, Mg
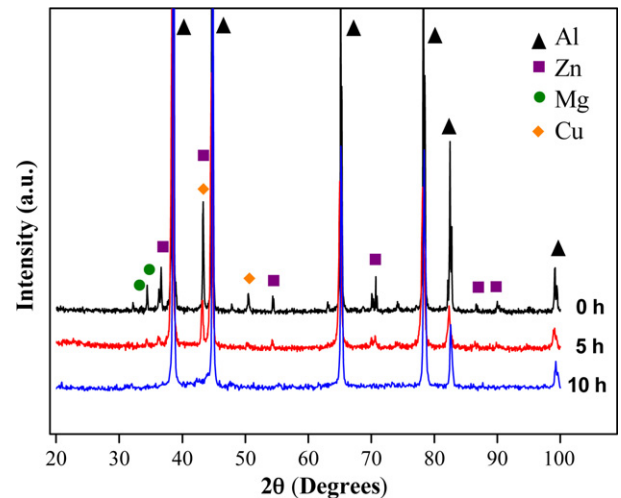

Fig. 2. XRD patterns of the Al$_{7075}$ powder mixture after selected milling times.

and Cu are clearly visible in the as-mixed sample (0 h of milling). After 5 h of milling, the intensity of those peaks decreases, which suggests that a portion of the alloying elements was dissolved into the Al matrix to form a solid solution. However, the characteristic reflections from alloying elements indicate that not all the Zn, Mg and Cu are in the solution. After 10 h of milling, the peaks of these elements almost disappear, since only the Al characteristic reflections are observed. This could be due to the dissolution of the alloying elements or to the very small particle size from elemental powders that they make their detection by XRD difficult. Additionally, the mechanical deformation introduced in the powder causes the particle and crystallite refinement (e.g. at 5 h of milling the crystallite size was reduced from 92 nm in the reference sample to 43 nm).

It was found that the position of the Al diffraction lines was shifted slightly to different angles for longer milling times. These variations were both, to lower and higher angles with respect to the reference material, and this has a direct effect in the lattice parameter value [12–14]. At 5 h of milling the Al diffraction lines were shifted to lower angles of the spectrum, and the lattice parameter increased slightly, compared with the reference sample. After 10 h of milling the diffraction lines of Al were shifted to higher angles, and the lattice parameter decreased. These variations are due to the MA process that generates severe plastic deformation in the powder and, as a consequence, structural defects (dislocations, vacancies and internal stresses) are formed and eliminated, affecting directly the lattice parameter value [12]. During the milling process, the dissolution of alloying elements that have different atomic radii (smaller and bigger than aluminum atomic size), has a direct effect on the lattice parameter of Al matrix. For example, a reduction in lattice parameter is the result of the dissolution of Zn and Cu, while Mg dissolution produces an increment in the lattice parameter [13,14]. The combination of both effects causes a high disorder in the lattice parameter. Additionally it is well know that milling process causes generation and annihilation of structural defects, and this has a direct effect on lattice parameter size [10].

Fig. 3 presents the XRD spectra of the ~5 wt.% zinc composites after 5 h of milling. It can be observed that the addition of G produced broader peaks on XRD pattern of MA products, as reported previously [6,7]. When the G content was increased the diffraction line intensity from alloying elements was decreased. Similar results have been reported during the mechanical milling of pure aluminum with graphite particles [6].

Because of the additional effect of G as PCA and the mechanical deformation introduced in the powder, particle and crystallite refinement occurs, and the lattice strain increases, leading to a broadening of the XRD peaks and the consequent decrease in the
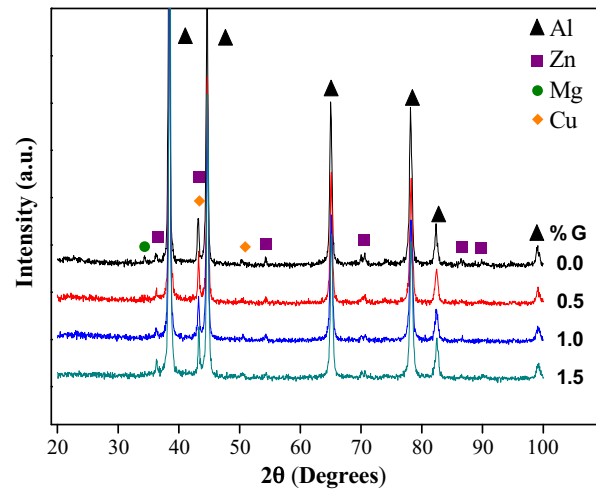

Fig. 3. XRD patterns of the Al_{7075} 5Zn composites after 5 h of milling with selected G contents.

peak intensities. Furthermore, if there exists dissolution of alloying elements into the aluminum matrix, the intensity of corresponding peaks could decrease and practically disappear [10,14].

Fig. 4 shows the XRD spectra of the ~4 wt.% zinc composites after the sintering and hot extrusion processes. No peaks corresponding to the alloying elements (Cu, Mg, Zn) and graphite were observed in any pattern. It can be deduced from the spectra that the milling process, the milling time (10 h), the sintering and hot extrusion processes promote both, the dissolution of alloying elements and the G dispersion. In addition, this figure shows the presence of the $MgZn_2$ phase and aluminum carbide (Al_4C_3), whose characteristic reflections are more evident as the G content increases. Moreover, it was observed that the G did not have a significant effect on the diffraction peaks shift of the matrix pattern.

3.3. Mechanical properties

Table 2 shows a comparison between the results of the tensile tests and Vickers microhardness measurements obtained for the composites and those reported in the literature for the Al_{7075}-O, Al_{7075}-T6 and Al_{7075}-T7 alloys.

By comparing experimental results with the reference sample (Al_{7075} 5Zn0G-M), it is observed that for 5 h of milling, the mechanical properties (σ_y, σ_{max} and μHV) did not change significantly for G contents between 0.0 and 0.5 wt.%. However for contents between 1.0 and 1.5 wt.%G, there is a small increment in the mechanical properties. In contrast, for 10 h of milling, all composites resulted

Table 1
Chemical composition and nomenclature used for the Al_{7075}-G composites synthesized in this work.

Sample	Composition (wt.%)								ρ_{Theor}
	Zn	Mg	Cu	Cr	Fe	Mn	G	Al	
Al_{7075} 5Zn0.0G	5.1	2.5	1.6	0.23	0.3	0.2	0.0	90.07	2.794
Al_{7075} 5Zn0.5G	5.1	2.5	1.6	0.23	0.3	0.2	0.5	89.57	2.791
Al_{7075} 5Zn1.0G	5.1	2.5	1.6	0.23	0.3	0.2	1.0	89.07	2.787
Al_{7075} 5Zn1.5G	5.1	2.5	1.6	0.23	0.3	0.2	1.5	88.57	2.783
Al_{7075} 4Zn0.0G	4.1	2.5	1.6	0.23	0.3	0.2	0.0	91.07	2.776
Al_{7075} 4Zn0.5G	4.1	2.5	1.6	0.23	0.3	0.2	0.5	90.57	2.773
Al_{7075} 4Zn1.0G	4.1	2.5	1.6	0.23	0.3	0.2	1.0	90.07	2.769
Al_{7075} 4Zn1.5G	4.1	2.5	1.6	0.23	0.3	0.2	1.5	89.57	2.766
Al_{7075} 3Zn0.0G	3.1	2.5	1.6	0.23	0.3	0.2	0.0	92.07	2.759
Al_{7075} 3Zn0.5G	3.1	2.5	1.6	0.23	0.3	0.2	0.5	91.57	2.755
Al_{7075} 3Zn1.0G	3.1	2.5	1.6	0.23	0.3	0.2	1.0	91.07	2.752
Al_{7075} 3Zn1.5G	3.1	2.5	1.6	0.23	0.3	0.2	1.5	90.57	2.748
Al_{7075}-O	5.1–6.1	2.1–2.9	1.2–2.0	0.18–0.28	≤0.50	≤0.30	0.0	Bal.	2.810

Table 2
Mechanical properties obtained in the extruded composites as a function of the milling time and composition.

Sample	Milling Time (h)	σ_y (MPa)	Variation (%)	σ_{max} (MPa)	Variation (%)	Strain (%)	Variation (%)	Vickers μ hardness	Variation (%)
Al$_{7075}$ 5Zn0G–M	0	256.5	–	349.5	–	7.2	–	90.0	–
Al$_{7075}$ 5Zn0.0G	5	280.0	9.2	368.5	5.4	7.4	3.5	83.0	−7.8
Al$_{7075}$ 5Zn0.5G	5	265.5	3.5	330.0	−5.6	5.7	−20.3	92.0	2.2
Al$_{7075}$ 5Zn1.0G	5	295.5	15.2	366.0	4.7	4.5	−37.1	97.0	7.8
Al$_{7075}$ 5Zn1.5G	5	376.0	46.6	413.0	18.2	2.9	−59.4	113.0	25.6
Al$_{7075}$ 4Zn0.0G	5	228.0	−11.1	319.0	−8.7	8.1	13.3	80.0	−11.1
Al$_{7075}$ 4Zn0.5G	5	235.5	−8.2	313.5	−10.3	6.2	−13.3	90.0	0.0
Al$_{7075}$ 4Zn1.0G	5	281.5	9.7	344.0	−1.6	3.7	−48.3	97.7	8.6
Al$_{7075}$ 4Zn1.5G	5	320.0	24.8	386.0	10.4	4.1	−42.7	111.8	24.2
Al$_{7075}$ 3Zn0.0G	5	211.5	−17.5	310.5	−11.2	9.8	37.1	80.0	−11.1
Al$_{7075}$ 3Zn0.5G	5	275.5	7.4	339.0	−3.0	4.3	−39.9	96.0	6.7
Al$_{7075}$ 3Zn1.0G	5	288.0	12.3	354.0	1.3	4.3	−39.9	101.0	12.2
Al$_{7075}$ 3Zn1.5G	5	302.0	17.7	385.5	10.3	4.7	−34.3	101.5	12.8
Al$_{7075}$ 5Zn0.0G	10	365.0	42.3	437.0	25.0	5.4	−24.5	127.0	41.1
Al$_{7075}$ 5Zn0.5G	10	305.0	18.9	400.0	14.4	7.2	0.0	100.0	11.1
Al$_{7075}$ 5Zn1.0G	10	382.0	48.9	452.0	29.3	5.1	−28.7	120.0	33.3
Al$_{7075}$ 5Zn1.5G	10	446.0	73.9	520.0	48.8	3.4	−52.4	141.0	56.7
Al$_{7075}$ 4Zn0.0G	10	315.0	22.8	397.0	13.6	9.4	31.5	115.0	27.8
Al$_{7075}$ 4Zn0.5G	10	360.0	40.4	430.0	23.0	5.5	−23.1	116.0	28.9
Al$_{7075}$ 4Zn1.0G	10	362.0	41.1	426.0	21.9	3.6	−49.7	128.0	42.2
Al$_{7075}$ 4Zn1.5G	10	428.0	66.9	463.0	32.5	2.4	−66.4	139.0	54.4
Al$_{7075}$ 3Zn0.0G	10	305.0	18.9	380.0	8.7	8.5	18.9	100.0	11.1
Al$_{7075}$ 3Zn0.5G	10	390.0	52.0	460.0	31.6	5.7	−20.3	127.0	41.1
Al$_{7075}$ 3Zn1.0G	10	389.0	51.7	452.0	29.3	4.1	−42.7	126.0	40.0
Al$_{7075}$ 3Zn1.5G	10	451.0	75.8	540.0	54.5	3.8	−46.9	149.0	65.6
Al$_{7075}$-O	0	96.5	−62.4	221.0	−36.8	16	122.2	–	–
Al$_{7075}$-T6	0	503.0	96.1	572.0	63.7	11	52.8	175.0	94.4
Al$_{7075}$-T7	0	435.0	69.6	505.0	44.5	13	80.6	155.0	72.2

with better mechanical properties than those observed in the reference sample, with increments in the G content. It was observed that for a constant content of Zn and G, the higher milling time resulted in higher mechanical properties (Table 2). Indeed, for the Al$_{7075}$ 5Zn1.5G sample with 5 h of milling, the σ_y, σ_{max} and μHV were 376 MPa, 413 MPa and 113, respectively, while for 10 h the values obtained were 446 MPa, 520 MPa and 141, respectively.

Fig. 5 shows the results of the yield strength (σ_y) and maximum strength (σ_{max}) of the Al$_{7075}$ 5Zn1.5G composite as a function of the milling time. Both curves σ_y and σ_{max} present a positive slope, indicating that G have a strengthening effect on the aluminum alloy matrix. Comparing the results to the reference sample, the yield
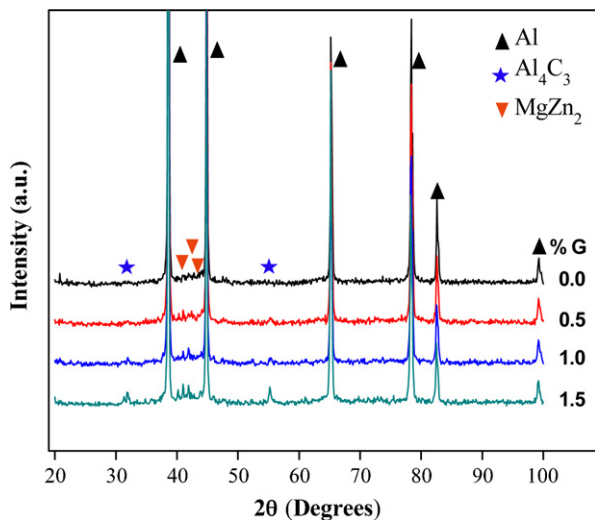

Fig. 4. XRD patterns of the Al$_{7075}$ 4Zn composites processed by MA for 10 h and hot extrusion at 773 K. The effect of the G addition can be observed as they promote the precipitation of the MgZn$_2$ phase and the crystallization of Al$_4$C$_3$.
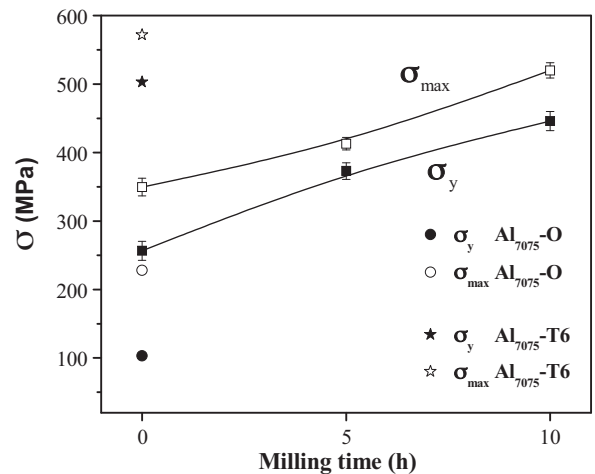

Fig. 5. Yield strength σ_y and the maximum strength σ_{max} of the Al$_{7075}$ 5Zn1.5G sample in the as-extruded condition, as a function of the milling time.

strength (σ_y) increased 46.6% and 73.9% after 5 and 10 h of milling, respectively. However, when comparing these results with data reported in the literature [15] for the Al$_{7075}$ alloy in the as-annealed condition (Al$_{7075}$-O), the σ_y increased 289.6% and 362.2% after 5 and 10 h of milling, respectively. The σ_{max} presented a similar behavior. This suggests that, in general, all the composites reported here have better properties than the Al$_{7075}$-O alloy. In MA, the milling time is one of the most important parameters [14]. When increasing the milling time the powder particles became harder due to the accumulation of strain energy, producing a stronger consolidated material after a hot extrusion process. Also, longer milling time favors the homogeneous dispersion of the graphite particles.

Additionally, in the MMC materials, the reinforcement particles strengthen the metal matrix both extrinsically, by load transfer
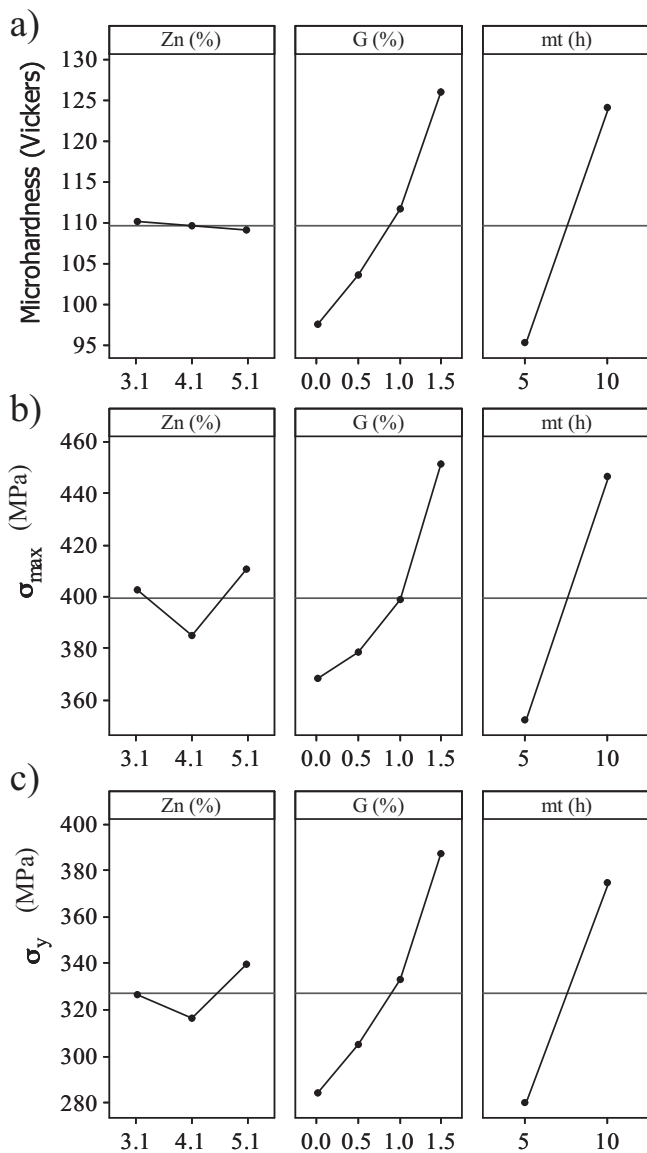
a)

b)

c)

Fig. 6. Main effect plots, showing the processing parameters vs. mechanical properties.

Fig. 7. Bright field TEM micrograph of the Al_{7075} 5Zn1.0G composite, showing the presence of Al_4C_3 (white arrow) and the $MgZn_2$ phase (dashed white arrow).

to the reinforcement, and intrinsically, by increasing dislocation density.

At 10 h of milling the process reaches a steady state, in this point the G are homogeneously distributed and the matrix transfers to the particles a part of the applied stress, which takes a fraction of the load. On the other hand, during the production of these composites, both the reinforcement particles and the matrix are heated to the processing temperature, reaching the thermomechanical equilibrium. During cooling, the thermal contraction of the Al matrix is much greater than that of the reinforcement particles (the Al and graphite thermal expansion coefficients are around $23.6 \times 10^{-6}\,\text{K}^{-1}$ and of $\sim10^{-6}\,\text{K}^{-1}$, respectively), which leads to a geometric mismatch. At the graphite-metal interphase, this geometrical disparity creates mismatch strains that are relieved by the generation of dislocations in the matrix. According to this, a decreasing of Zn content up to 3.1% in samples milled during 10 h can be compensated by the addition of graphite particles.

In order to determine the effects of Zn content, G and milling time on the mechanical properties of the composites, a statistical
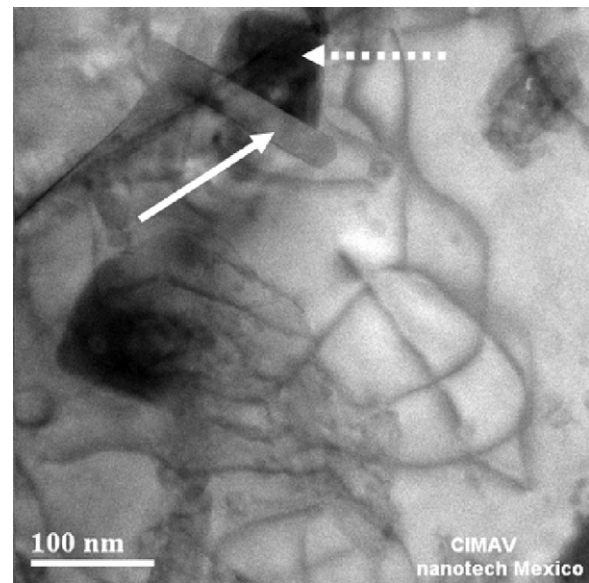
Anova two-way analysis was carried out. From the obtained results, it can be observed that mechanical properties are mainly affected by milling time (mt) and G addition, and in a lesser extent by the additions of Zn, as shown in Fig. 6.

In addition, on looking trough the data in Table 2, it can be observed that the composites prepared with 10 h of milling present mechanical properties very similar to or higher than those of the Al_{7075} alloy in the T7 condition. This opens the possibility to investigate the effect of aging heat treatments on the mechanical properties of this kind of composites. Nevertheless, the milling time and mainly the addition of graphite particles, cause a decrement in elongation, property that could be improved by a heat treatment. Additionally, it can be seen in Table 1 that the theoretical density (ρ_{Theor}) of the composites decreased as a function of the Zn and G content, which must have a considerable effect on the resistance/weight ratio.

4. Discussion

The principal alloying element in the Al_{7075} alloy is Zn, whose contribution is the solid solution and precipitation strengthening under the T6 temper. This element presents a high density value ($7.14\,\text{g/cm}^3$), which has repercussion on the Al_{7075} density value. From Table 2 it is observed that G additions and milling time have a positive effect on the studied mechanical properties; consequently, there is the possibility of obtaining stronger and lighter materials for potential structural applications.

The results presented in the previous section suggest that several reinforcement mechanisms might explain the improvement on the mechanical properties of the synthesized composites. To fully understand the strengthening mechanisms caused by graphite dispersion in the Al-based composites, additional experiments are required. However, the enhancement of mechanical properties is due mainly to the load transfer and the thermal mismatch, moreover, the following hypotheses can be considered: (i) precipitation of $MgZn_2$, (ii) formation of Al_4C_3, (iii) dispersion of Al_2O_3 during the milling process, (iv) inhibition of dislocation motion by $MgZn_2$, Al_4C_3, and Al_2O_3 and (v) crystallite refinement by the milling process.

The XRD spectra displayed in Fig. 4 illustrate that the G addition has no effect on the $MgZn_2$ phase precipitation sequence in composites with constant Zn content, but it favors the crystallization of the Al_4C_3 phase, formed during the sintering process and/or the hot extrusion process. Furthermore it is evident that high G concentration improves the formation of hard Al_4C_3 phase, which overcompensates the decreasing on mechanical properties caused by reduction in Zn content. These precipitates ($MgZn_2$ phase and aluminum carbide, Al_4C_3) are responsible of the aluminum based composite reinforcement, which seems to corroborate the hypotheses (i) and (ii). The hypothesis (iii) involves the dispersion of aluminum oxide during milling; although there is no evidence of the Al_2O_3 phase in the XRD patterns (Fig. 4), its presence cannot be avoided. It is feasible the formation of a brittle oxide layer on the aluminum elemental powder surface and this layer is broken during the milling process and dispersed into the aluminum matrix. The fourth hypothesis is related to the interrupted dislocations motion due to the presence of a second phase. It is expected from Fig. 4 that $MgZn_2$, Al_4C_3 and the probable presence of Al_2O_3, affect the dislocations movement. Fig. 7 shows a representative bright field TEM image of the Al_{7075} 5Zn1.0G composite. Additional to the bend contours and grain boundaries, notice the presence of Al_4C_3 (indicated by a white arrow) and a dark phase identified as the $MgZn_2$ phase (showed by a dashed white arrow).

The fifth mechanism is associated to the crystallite refinement by the mechanical milling process, and its effect in the increment on the mechanical properties in the as-extruded samples. Crystallite refinement by milling process has a direct relationship with the milling time. During the posterior sintering and hot extrusion stages. There exist a grain growth, however, crystal size was kept in the range of 1–4 hundreds nm.

The five strengthening mechanisms briefly explained above suggest that there is more than one mechanism that causes the enhancement of the Al_{7075} composites mechanical properties. However, a deeper and more careful analysis is needed to corroborate these strengthening mechanisms and to confirm previous studies reported elsewhere [15].

5. Conclusions

Al_{7075} alloy from elemental powder and dispersion of G have been synthesized simultaneously by milling process. The mechanical properties (σ_y, σ_{max}, μHV) of the composites synthesized in this work were considerably higher than those of the plain Al_{7075} alloy (Al_{7075}-O, Table 2). Zinc is an alloying element that has an important effect on the mechanical properties in Al-Zn alloys: as the Zn content decreases, the mechanical properties decrease. Graphite particles may contribute in the Zn reduction of the Al_{7075} alloys, with the inherent decrease in the composites density. The improvement on mechanical properties of the Al_{7075} composites can be explained by different strengthening phenomena.

References

[1] ASM Handbook, vol. 21, Composites, 2001.
[2] B. Prabhu, C. Suryanarayana, L. An, R. Vaidyanathan, Mater. Sci. Eng. A 425 (2006) 192–200.
[3] N. Zhao, P. Nash, X. Yang, J. Mater. Proc. Technol. 170 (2005) 586–592.
[4] S.M. Zebarjad, S.A. Sajjadi, Mater. Des. 28 (2007) 2113–2120.
[5] J.B. Fogagnolo, F. Velasco, M.H. Robert, J.M. Torralba, Mater. Sci. Eng. A 342 (2003) 131–143.
[6] M.I. Flores-Zamora, I. Estrada-Guel, J. González-Hernández, M. Miki-Yoshida, R. Martínez-Sánchez, J. Alloy Compd. 434–435 (2007) 518–521.
[7] I. Estrada-Guel, C. Carreño-Gallardo, D.C. Mendoza-Ruiz, M. Miki-Yoshida, E. Rocha-Rangel, R. Martínez-Sanchez, J. Alloy Compd. 483 (2009) 173–177.
[8] E.M. Ruiz-Navas, J.B. Fogagnolo, F. Velasco, J.M. Ruiz-Prieto, L. Froyen, Compos. Part A 37 (2006) 2114–2120.
[9] G.K. Williamson, W.H. Hall, Acta Metal. 1 (1953) 22–31.
[10] B.D. Cullity, S.R. Stock, Elements of X-Ray Diffraction, third ed., 2001.
[11] R. George, K.T. Kashyap, R. Rahul, S. Yamdagni, Scripta Mater. 53 (2005) 1159–1163.
[12] D. Oleszak, V.K. Portnoy, H. Matyja, Mater. Sci. Forum 312–314 (1999) 345–350.
[13] M. Tavoosi, F. Karimzadeh, M.H. Enayati, Mater. Lett. 62 (2) (2008) 282–285.
[14] C. Suryanarayana, Prog. Mater. Sci. 46 (2001) 1–184.
[15] MatWeb-Online Materials Information Resource – www.matweb.com, 2009.